Polym. Bull. (2010) 64:221–231
DOI 10.1007/s00289-009-0138-8

Polypropylene nanocomposites using metallocene catalysts supported on commercial organophilic clays

Maria de Fátima Vieira Marques · Mônica Couto de Oliveira

Received: 26 March 2009 / Revised: 8 July 2009 / Accepted: 14 July 2009 /
Published online: 25 July 2009

Abstract In this work, different organophilic clays were employed as supports for the preparation of heterogenized metallocene catalysts to be evaluated for propylene polymerization. The supports employed were Viscogel B8, Claytone HY and Cloisite 15A. These supports were chemically pre-treated with methylaluminoxane (MAO) and then impregnated with $SiMe_2(2\text{-Me-Ind})_2ZrCl_2$ complex. The prepared catalysts performed much worse than the homogeneous precursor system. Those organoclays, as well as the prepared metallocene catalysts, were analyzed by X-ray diffractometry (XRD), showing the displacement and broadening of the clay peak to lower angles. The polymers were also characterized by XRD, infrared absorption spectrometry (FTIR) to determine the isotactic index, by thermogravimetric analysis (TGA) to determine the degradation temperatures, by differential scanning calorimetry (DSC) to determine the thermal characteristics of the polypropylene produced, and by transmission electron microscopy (TEM) to examine the morphology of the materials obtained.

Keywords Polypropylene · Propylene polymerization · Organophilic clays · Supported metallocene catalysts

Introduction

Metallocene catalysts have paved the way for a new area in polymerization of olefins and can provide new polymer structures and resulting properties in comparison to the traditional Ziegler catalysts [1]. The advantages of the use of metallocene catalysts are well known and fully reported in the scientific literature [2].

M. de Fátima Vieira Marques (✉) · M. C. de Oliveira
Instituto de Macromoléculas/IMA, Universidade Federal do Rio de Janeiro, UFRJ, CP 68525, CEP 21941-590 Rio de Janeiro, RJ, Brazil
e-mail: fmarques@ima.ufrj.br

The use of metallocene catalysts in industrial processes for olefin polymerization is regarded as a revolutionary step in the history of polymers, and has been investigated for over 20 years. The number of publications in the areas of synthesis and applications of metallocene polyolefins has grown rapidly in recent decades. Metallocene complexes exhibit high catalyst activities and stereospecificity. Additionally, they are soluble in hydrocarbons (homogeneous catalysis), have virtually only one type of active site (single site catalyst) and their chemical structures can be easily modified when compared to the Ziegler catalysts. The properties of the resultant polyolefins may be provided through the structure of the catalyst used during its synthesis. Control of molar mass, narrow molar mass distribution and structural interchain uniformity related to comonomer content and tacticity can be achieved by careful selection of reaction conditions. The catalytic activity of metallocene systems is 10–100 times higher than that of conventional Ziegler catalysts for olefin polymerization [2–7].

Among polyolefins, polypropylene (PP) is one of the most used plastics in various applications. However, to overcome some disadvantages of PP, such as low temperature and low tenacity in service, their properties have been improved with nanotechnology [8].

PP has a great potential for composites and nanocomposites, since it can be processed by conventional technologies such as injection molding and extrusion. The properties of PP are enhanced by introducing micro and nanofillers, resulting in composites with high rigidity and tenacity. PP is widely used in the automobile industry; therefore polypropylene/clay nanocomposite (PPCN) is a very attractive material with high-value added applications. The development of polymer/clay nanocomposites is the most recent evolutionary step in the art of polymers. Thus, nanocomposites have great potential to diversify the applications of conventional polymer materials [9–15].

Research on polymer/organoclay nanocomposites has progressed greatly in the past decade, due to their potential as alternative low-cost and high-performance composites, for applications ranging from automobiles, food packaging and even biomedical engineering. This polymer/clay hybrid belongs to a new class of materials including nanolayers of aluminium phylosilicate as filler, where it is evenly dispersed in the polymer matrix, resulting in materials with unusual properties. Because of its extremely high aspect ratio (length/thickness) when the clay structures are delaminated during processing, the polymer properties can be improved, even with a moderate load (less than 5 wt.%), compared to conventional composites, which employ loads as higher as 20–40 wt.%. The high aspect ratio allows transfer of energy from one stage to another. Typically, mechanical performance, thermal stability, barrier properties, chemical resistance and flame retardant properties are increased without any loss in processing due to low density. It is also an easy material to recycle. The improvement of its properties is due to the synergistic effects of nanoscale structure, which maximizes the interactions between load and polymer molecules [16–18].

The most important techniques to prepare PP/Clay nanocomposites involve melt intercalation or in situ polymerization by fixation of the catalyst components in the interlayer space of the clay. Through this last method, in situ propylene

polymerization can actually take place between the silicate layers, leading not only to PP with a high isotacticity and molecular weight, but also to a highly exfoliated structure even at high clay content levels.

The present work studies the preparation of an isospecific metallocene catalyst supported on different commercial clays and their performance for propylene polymerization.

Experimental

Materials

All reagents were handled under a nitrogen atmosphere using the Schlenk technique. Propylene (Rio Polímeros, Brazil, polymerization grade) and nitrogen (W. Martins, Brazil, 99.9%) were purified by sequential passage through columns containing 4 Å molecular sieve and copper catalyst to remove oxygen, carbon dioxide and moisture. Toluene was refluxed over metallic sodium/benzophenone and was distilled under a nitrogen atmosphere prior to use. Methylaluminoxane (MAO) (10 wt.% solution in toluene (Chemtura, Germany) and $SiMe_2(2\text{-Me-Ind})_2ZrCl_2$-dimethyl silyl bis (2-methyl-Indenil) zirconium dichloride (Boulder Sci. USA) were used without further purification. The commercial organophilic clays used as supports were: Claytone HY (Bentonit União Nordeste, Brazil); Cloisite 15A (Southern Clay, USA); and Viscogel B8 (Bentec Rheol). Add., Italy. All organoclays were used without further purification.

Support chemical pre- treatment

A solution of MAO in toluene was added slowly to Schlenk bottle with about 2.5 g of dry support, under a nitrogen atmosphere, remaining under magnetic stirring for 4 h at room temperature. Then, there were successive washes with toluene to remove excess of unreacted MAO.

Preparation of supported catalyst

A solution of the catalyst $SiMe_2(2\text{-Me-Ind})_2ZrCl_2$ in toluene was prepared under nitrogen. This catalyst solution was mixed with the MAO-pre-treated support. The concentration of metallocene on the support was set at 0.05 mmol/g. In the case of homogeneous catalyst, the prepared solution of $SiMe_2(2\text{-Me-Ind})_2ZrCl_2$ in toluene was added directly to the propylene polymerization.

Polymerization

Heterogeneous propylene polymerization was carried out in a 1,000-ml glass reactor. MAO was used as cocatalyst (Al/Zr = 1,000). The reagents were added into the reactor at 60 °C in the following order: 100 ml toluene, MAO solution and propylene. After saturation of propylene (1 bar) under 600 rpm, the supported

catalyst suspension was injected into the reactor so that the Zr concentration was 0.005 mmol and the propylene pressure was increased to 2 bar, initiating polymerization. The reaction was interrupted after 1 h and the product was transferred to a solution of HCl/ethanol. After 24 h under magnetic stirring, the polymer was filtered, washed with $NaHCO_3$ solution and ethanol, and dried at 60 °C to constant weight.

The homogeneous polymerization was carried out by a similar method as the heterogeneous one. After charging the reactor with toluene, MAO solution and propylene, a solution of the catalyst in toluene was then injected into the reactor, starting the polymerization. All the reaction conditions were the same as the polymerization with the supported catalyst.

Support and catalyst characterization

The chemical characteristics of the organoclays and catalysts were evaluated through X-ray diffractometry (XRD), measured in the Rigaku—Miniflex model, working with a potential difference of the tube at 30 kV and electrical current of 15 mA. The scan was performed in the range of 2θ from 2 to 30°, with a goniometer speed of 0.05°/min. X-Ray diffraction patterns were recorded with a CuKα radiation at $\lambda = 1.5418$ Å.

Polymer characterization

Differential scanning calorimetric analyses (DSC) were used to determine the polymer melting temperature and degree of crystallinity. The analyses were carried out in a TA Instruments model Q1000 instrument. The samples were heated in the temperature range of 40–200 °C at a heating rate of 10 °C/min. The material underwent two heating procedures, the first to erase the thermal history of the synthesized polymer. The standard substance for calibration of the DSC apparatus was indium. The melting temperature and the melting enthalpy were calculated from the thermograms obtained during the second scan. The melting enthalpy values were used to estimate the degree of crystallinity of each material using 209 J/g as the theoretical value for ΔH_m of a completely crystalline polypropylene [19, 20].

Infrared absorption spectroscopy (FTIR) was used to analyze the stereospecificity of the polymers obtained. Spectra were obtained with 50 scans and resolution of 4 cm^{-1}, in the range of 4,000–400 cm^{-1}.The relationship of the absorption bands at 998 cm^{-1} (related to the alpha-helical conformation of isotactic sequences) and 973 cm^{-1} as internal standard was employed and the isotactic index (I.I.) was calculated according to $A_{998}/A_{973} = 1.08$ I.I.–0.15.

The synthesized polypropylenes were also characterized by X-ray diffractometry (XRD), using the same method and equipment as for the catalysts and the organoclays.

The degradation temperatures of the polymers were analyzed by thermogravimetry (TGA), in a TA Instruments model Q500. The samples were heated in the temperature range from room to 700 °C, in an inert atmosphere, with a heating rate of 10 °C/min.

Transmission electron microscopy (TEM) was used to examine the morphology of filler and its distribution in the polymer matrix. For the analysis of TEM, the sample was melted in a heating plate in a mold and then cooled to room temperature to form a molded sample. This sample was then cut with a glass knife in an ultramicrotome at the angle of 6° at room temperature. The thickness was about 70 nm. The cut was placed in a copper grid until examination in the electron microscope.

Results and discussion

Table 1 shows the degradation temperatures T_{onset} and T_{max}, as well as the total weight loss up to 700 °C obtained from the TGA analyses of the organoclays used as different supports for the $SiMe_2(2\text{-Me-Ind})_2ZrCl_2$ metallocene catalyst.

As can be seen from Table 1, Cloisite 15A has the highest amount of organic material in the interlamelar space and the lowest degradation temperature compared to the other organoclays.

Table 2 shows the polymerization results and the calculated activities for the homogeneous system and the prepared supported catalysts in propylene polymerization using MAO as cocatalyst. There was a sharp drop in the catalytic activity in comparison with that of the homogeneous one for all the evaluated supported systems. The clay content in the materials obtained was above 8 wt.%, and in the case of using Cloisite 15A as support, the material consisted mostly of clay with a small amount of polypropylene. This result can be explained due to the type of ammonium salt in this clay, which contains two long alkyl chains causing sterical

Table 1 Thermogravimetric analyses of clays used as supports for metallocene catalyst

Clay	Ammonium cation	Catalyst	$T_{on\ set}$ (°C)	T_{max} (°C)	Weight loss (%)
Viscogel B8	Trimethyl-octadecyl	1	251	331	34
Cloisite 15A	Dimethyl-diHT	2	224	266	39
Claytone HY	Dimethyl-benzyl-HT	3	234	303	38

HT hydrogenated-tallow (~65% C18; ~30% C16; ~5% C14)

Table 2 Polymerizations performed in toluene at 60 °C cocatalyzed by MAO

Catalyst	Clay	Yield (g)	Catalyst activity (tonPP/molZr*h)	Clay content (wt.%)[a]
1	Viscogel B8	1.24	248	8
2	Cloisite 15A	0.06	12	100
3	Claytone HY	0.41	82	24
Homogeneous	–	71.48	14,297	–

[a] Theoretical content of clay, considering the yield and the amount of catalyst added; Reaction conditions: temperature = 60 °C; $P_{propylene}$ = 2 bar; pre-contact time = 15 min.; reaction time = 60 min., [Zr] = 50 μm [Al]/$[Zr]_{MAO}$ = 1,000

hindrance in the interlamelar space, thus making it difficult for the metallocene complex to be fixed in the galleries of this support. On the other hand, the less bulky ammonium salt in Viscogel B8 could be the reason why the highest catalyst activity was obtained when using this clay as metallocene support.

Figures 1, 2 and 3 show the X-ray diffractograms of clays, catalysts and polypropylenes obtained from the polymerizations with the heterogeneous systems. The peak related to the clay interlamelar spacing in the range of 2θ lower than 10° for each organoclay is used as indication of obtaining polymer nanocomposites, through the displacement of the basal peak to lower angles and/or the decrease of its intensity.

In Fig. 1, the clay used as catalyst support was Viscogel B8, which has 2 peaks at $2\theta = 3.7$, and 7.2°, identified as the (001) and (002) diffraction peaks. The (00*l*) peaks represent the reflections due to the stacks of the clay layers. The shift of those peaks in the XRD pattern thus reflects changes in distance between the silicate platelets. The initial *d*-spacing of the organoclay was determined to be between 2.4 and 2.6 nm. In the XR diffractograms of the clay and the catalyst prepared with this silicate, a peak can be found at 2θ (approximately 20°). This peak represents the (110) reflection of the montmorillonite. The (*hk*0) plane characterizes the atomic arrangement in the plane that is parallel to the *z*-axis. This peak is therefore independent of the distance between silicate platelets, and its location can be used as a reference.

XRD profile of the metallocene catalyst supported onViscogel B8 did not show any peak at the lower angle (d001 diffraction peak). The lowest angle that we could measure in our XRD technique is $2\theta = 2°$, which correlates with a *d*-spacing of

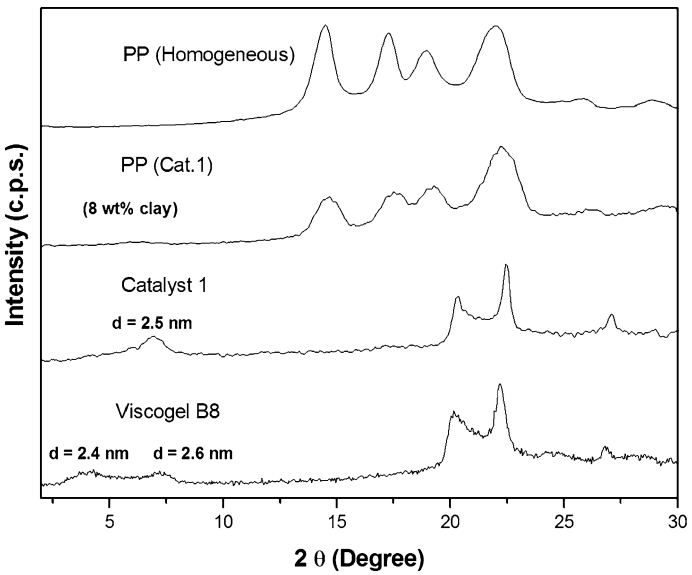

Fig. 1 X-ray diffractograms of Viscogel B8, catalyst 1 and polypropylene obtained with the supported metallocene catalyst 1 and that synthesized using the homogeneous system

4.4 nm. In addition, the (002) diffraction signal shifted toward a lower angle and also became broader. This may occur particularly if the platelets show a significant distribution in layer distances, rather than a stronger, sharper peak due to repeated distances of the same length. This is an indication that the catalyst components have been intercalated in the clay layers, which is very important to initiate the polymerization between clay platelets to produce PP nanocomposite. In fact, with the polymerization of propylene using this catalyst, the (002) peak in PP disappeared in the range that can be examined using WAXS, leading to a well-exfoliated PP/clay structure containing 8 wt.% of silicate in the nanocomposite.

For comparison, the XRD pattern of the PP obtained by the homogeneous metallocene catalyst is also presented in Fig. 1. The polypropylene presents diffraction peaks at $2\theta = 13.9$; 16.8; 18.4 and 21.8° corresponding respectively to the planes (110), (040), (130) and (111) of its crystalline α-phase. On the other hand, the X-ray diffraction spectra of the PP/clay nanocomposite indicated that although the crystalline form of the matrix was still essentially the α-crystal type, the diffraction peaks at 13.9; 16.8; 18.4 decreased and that of 21.8° broadened. This phenomenon indicates that the presence of nanoclay made the crystal phase of the PP change to some extent, that is, there was an interaction of clay layers with the macromolecular chains of PP, so the nanoclay particles and PP matrix were compatible.

Figure 2 shows the characteristic diffraction of clay Cloisite 15A, where a single peak at $2\theta = 7.6°$ appears and is correlated to the (002) diffraction peak. The basal reflection d(001) did not appear in this analysis. The (002) reflection represents half-length of the actual average distance between two silicate layers, whose interplanar

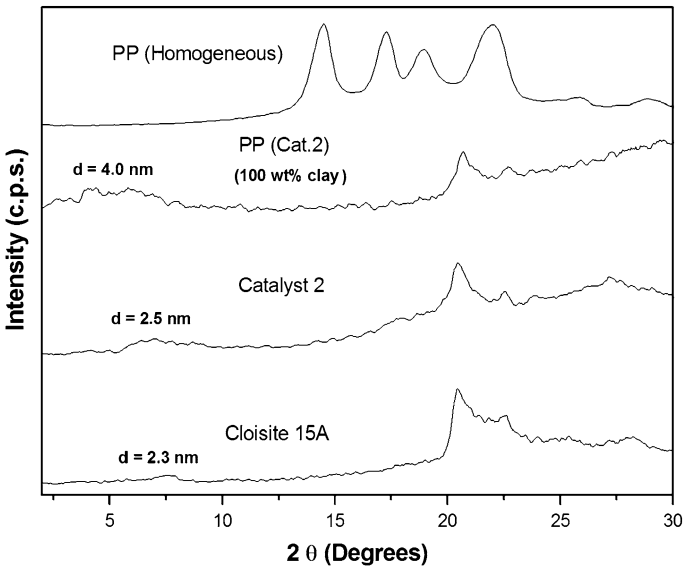

Fig. 2 XR diffractograms of Cloisite 15A, catalyst 2 and the polypropylenes obtained with the supported catalyst and the homogeneous one

distance was calculated to be around 2.3 nm. Figure 2 shows that in fact the material obtained in the polymerization with the supported catalyst 2 did not show any characteristic diffraction of polypropylene crystals, although the second-order reflection d(002) of this smectite visibly shifted to lower angles and became very broad. Moreover, the second-order peak of catalyst 2 was also slightly shifted to lower angles and also broadened in comparison with the original clay. It is possible that some polypropylene molecules were produced, increasing the interlamelar distance of the clay layers at the end of polymerization.

Regarding the use of Claytone HY (Fig. 3) as the metallocene catalyst support, a very similar XRD pattern was obtained in the analysis, where only the d(002) reflection appeared at the same angle ($2\theta = 7.6°$) as Cloisite 15A. In catalyst 2E, there was a peak shift to $2\theta = 6.1°$ with the broadening of the reflection in this range. Once again this indicates that the interplanar distance of the clay increased by incorporating the catalyst's components. Analysis of the XRD diffractogram of the polymer produced containing 24 wt.% of clay shows a peak at $2\theta = 6.3°$ (2.8 nm) and the beginning of a peak below $2\theta = 2°$, indicating the intercalation of the polymer matrix between the clay lamellae or even the exfoliation of part of the clay.

Table 3 shows the results of infrared spectrometry, differential scanning calorimetry and thermogravimetric analyses of the polypropylenes obtained in this study. The DSC results confirm that the material obtained with catalyst 2 (whose support is Cloisite 15A) does not contain crystalline PP, as shown in the X-ray diffractometry and verified by the absence of PP endotherm. Moreover, the low temperatures of degradation are due to the organic material contained in the clay and/or the production of PP oligomers. It can be observed that the amount of volatile

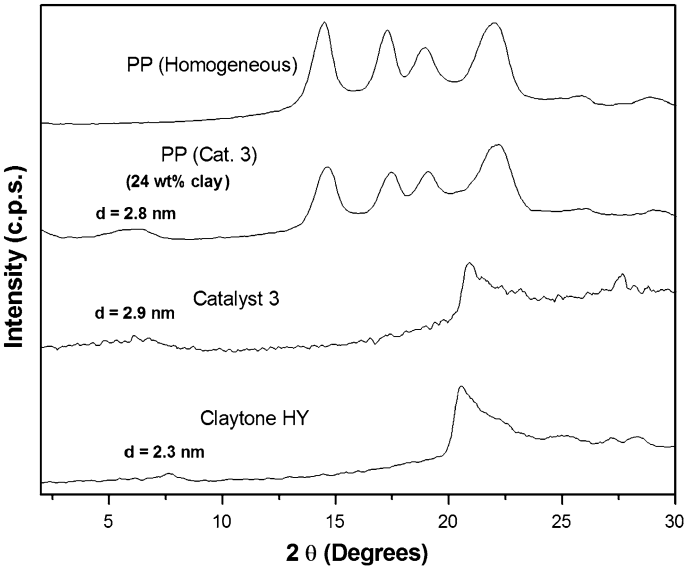

Fig. 3 Diffractograms of Claytone HY, catalyst 3 and polypropylenes obtained with the supported catalyst and the homogeneous one

Table 3 Characteristics of polypropylenes obtained with the $SiMe_2(2\text{-Me-Ind})_2ZrCl_2$ catalyst in homogeneous phase and supported on clays

Catalyst	Isotacticity index (%)[a]	T_{onset} (°C)	T_{max} (°C)	T_c (°C)	T_m (°C)	ΔH_m (J/g)	X_c (%)	Residual content (%)[b]
1	98.7	319	387	126	142	63	30	8
2	ND	231	240	ND	ND	ND	ND	49
3	100	282	328	117	144	63	30	12
Homogeneous	77.2	333	384	106	138	67	32	0.2

ND not detected

[a] Isotactic index (mm%), obtained by FTIR

[b] After heating up to 700 °C; X_c = crystallinity degree; T_{onset} e $T_{máx}$ = degradation temperature by TGA

material in the polymerization product was 51.4 wt.%, which is higher than that of the original clay.

Regarding the degradation temperature of the obtained PP, no enhancement of T_{onset} or T_{max} was observed for the composites in comparison with the PP obtained with the homogeneous catalyst.

On the other hand, the polymers obtained with the supported catalysts 1 (with Viscogel) and 3 (Claytone) showed higher melting temperatures (T_m), than the homogeneous PP. Similarly, the crystallization temperatures (T_c) increased for both corresponding PP nanocomposites. Thus, the PPs produced with these clay-supported catalysts showed higher isotactic indices compared with that obtained with the homogeneous system, although the crystalline degree decreased.

Figure 4 shows micrographs obtained through transmission electron microscopy of polypropylene synthesized with catalyst 1, using Viscogel B8 as support. It can be seen that the clay was well dispersed in the matrix, with exfoliated/intercalated morphology.

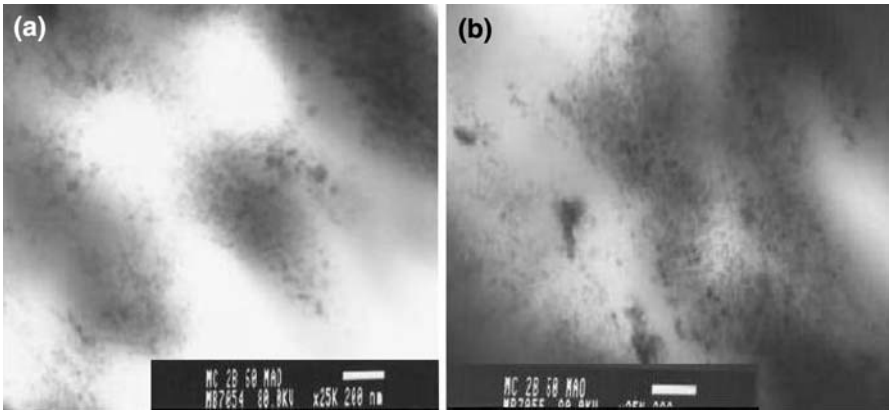

Fig. 4 (**a**) TEM Micrographs of PP nanocomposite synthesized by catalyst supported on Viscogel B8 with an increase of 25 K and (**b**) from another region

Conclusion

The activities of the catalysts based on $SiMe_2$ (2-Me-Ind)$_2ZrCl_2$ supported on different organophilic clays were much lower than that of the homogeneous system in propylene polymerization. The most effective catalyst was that supported on Viscogel B8, followed by Claytone HY and Cloisite 15A. The last was not a suitable support for this system under the employed conditions. The catalysts obtained after impregnation of the metallocene led to solids with higher interlayer space and broadened XR diffraction signals at angle ranges from lower than 10°. We also observed that the material synthesized with the catalyst supported on Claytone HY is a PP nanocomposite with high amounts of clay and mainly has an intercalated morphology, since the typical clay peak related to the interlamelar distance is shifted toward lower values of 2θ, below 2°. Besides this, the material synthesized with the catalyst supported on Viscogel did not present a peak in the range of low angles, indicating the formation of exfoliated PP nanocomposites. The temperatures of crystallization (T_c) and melting (T_m) of the polymers obtained with the clay supported system were higher than those of the homogeneous one. The transmission electron microscopy analysis of the polypropylene nanocomposite obtained with the catalyst supported on Viscogel showed that the clay was well dispersed in the polymer matrix.

Acknowledgments The authors thank the National Research Council (CNPq), the Office to Improve University Research (CAPES) and Petrobras for supporting this work.

References

1. Wang W, Fan Z, Zhu Y, Zhang Y, Feng L (2002) Effects of cocatalyst on structure distribution of propylene polymers catalyzed by *rac-Me$_2$Si(Ind)$_2$ZrCl$_2$*/aluminoxane. Eur Polym J 38:1551–1558
2. Franceschini FC, Tavares TTR, Greco PP, Galland GB, Santos JHZ, Soares JBP (2005) Effects of the type and concentration of alkylaluminum cocatalysts on the molar mass of polypropylene made with in situ supported metallocene catalysts. J Appl Polym Sci 95:1050–1055
3. Kaminsky W (1995) Polymerization catalysis. Catal Today 62:23–34
4. Sinn H (1995) Macromol Symp 97:27–32
5. Kaminsky W, Laban A (2001) Metallocene Catal Appl Catal A Gen 222:47–61
6. Lisovskii A, Shuster M, Gishvoliner M, Lidor G, Eisen MS (1998) Polymerization of propylene by metallocene and Ziegler-Natta mixed catalytic systems: study of PP properties. J Polym Sci Part A Polym Chem 36:3063–3072
7. Wang B (2006) *Ansa*-metallocene polymerization catalysts: effects of the bridges on the catalytic activities. Coord Chem Rev 250:242–258
8. Ding C, Jia D, He H, Guo B, Hong H (2004) How organo-montmorillonite truly affects the structure and properties of polypropylene. Polym Test 24:94–100
9. Garcés JM, Moll DJ, Bicerano J, Fibiger R, McLeod DG (1999) Polymer nanocomposites for automotive applications. Adv Mater 12:1835–1839
10. Bergman JS, Chen H, Giannelis EP, Thomas MG, Coates GW (1999) Chem Commun 2179–2180
11. Kato M, Matsushita M, Fukumori K (1999) Development of a new production method for a polypropylene-clay nanocomposite. Polym Eng Sci 44:1205–1211
12. Nam PH, Maiti P, Okamoto M, Kotaka T, Hasegawa N, Usuki A (2001) A hierarchial structure and properties of intercalated polypropylene/clay nanocompósitos. Polymer 42:9633–9640
13. Tang Y, Hu Y, Song L, Zong R, Gui Z, Chen Z, Fan W (2003) Preparation and thermal stability of polypropylene/montmorillonite nanocomposites. Polym Degrad Stab 82:127–131

14. Minisini B, Tsobnang F (2005) Molecular dynamics study of specific interactions in grafted polypropylene organomodified clay nanocompósito. Compos Part A Appl Sci Manuf 36:539–544
15. Jordan J, Jacob KI, Tannenbaum R, Sharaf MA, Jasiuk I (2005) Experimental trends in polymer nanocomposites—a review. Mater Sci Eng A 393:1–11
16. Lew CY, Murphy WR, McNally GM (2004) Preparation and properties of polyolefin-clay nanocompósitos. Polym Eng Sci 44:1027–1035
17. Kim JH, Koo CM, Choi YS, Wang KH, Chung IJ (2004) Preparation and characterization of polypropylene/layered silicate nanocomposites using an antioxidant. Polymer 45:7719–7727
18. Pandey JK, Reddy KR, Kumar AP, Singh RP (2005) An overview on the degradability of polymer nanocompósitos. Polym Degrad Stab 88:234–250
19. Chaves EG (2005) The study of the binary metallocene catalysts performance and estimation of the polypropylene properties. Doctor Thesis, Instituto de Macromoléculas Professora Eloisa Mano, Universidade Federal do Rio de Janeiro, Brazil
20. Paukkeri R, Lehtinen A (1993) Thermal behavior of polypropylene fractions: 1. Influence of tacticity and molecular weight on crystallization and melting behavior. Polymer 34:4075–4082